Analysis of Corrugated Waveguides With a Set of Edge-Conditioned Vector Basis Functions

Smain Amari, Rüdiger Vahldieck and *Jens Bornemann
Swiss Federal Institute of Technology (ETH), Zürich, Switzerland
* Department of Electrical and Computer Engineering, Box 3055 University of Victoria B.C., Canada V8W 3P6

Abstract

The paper presents a rigorous fullwave analysis of corrugated circular waveguides. The propagation properties are determined from a classical eigenvalue problem with no recourse to space harmonics. A set of vector edge-conditioned basis functions is used to guarantee numerical efficiency. The speed of the method allows the accurate determination of the entire dispersion diagram of a large number of modes. Results are presented and compared with available data to demonstrate the efficiency and accuracy of the approach.

I. INTRODUCTION

Linear particle accelerators and slow-wave structures exploit the slow wave nature of periodic structures to guarantee efficient electromagnetic coupling. Corrugated circular waveguides are also important components in modern antenna feeds where a high degree of symmetry in the radiation pattern and a very low crosspolarisation are required [1], [2].

From a mathematical point of view, the invariance of the structure under a discrete translation by one period implies that the solutions of Maxwell's equations obey the Floquet condition [3].

Expansions in space harmonics is a popular approach for the analysis of corrugated waveguides [2]. A disadvantage of this approach stems from the fact that the propagation constant is eventually determined from a non-linear determinant equation. An iterative process requiring the repeated evaluation of a determinant is used; degenerate and closely located roots can pose a serious difficulty for such an approach. The formulation used in this paper is based on the Coupled-Integral Equation Technique (CIET) [4]. It allows the determination of the propagation constants from the *classical* eigenvalues of a generalized matrix eigenvalue problem. The dispersion diagram of a large number of modes can be determined accurately with minimal numerical effort. Applications of this approach have been reported in [5].

In this paper we use a set of edge-conditioned basis functions to investigate some important features of the dispersion diagrams of corrugated circular waveguides. We examine in detail the zero-thickness approximation where the thick corrugations are replaced by a zero-thickness iris.

0-7803-4900-8/98/$10.00

II. THEORY

The structure under consideration is depicted in Figure 1. It consists of a lossless corrugated circular waveguide of radius a. The inner radius of the corrugations of thickness t is b. The periodicity of the corrugations is p. Since the structure is

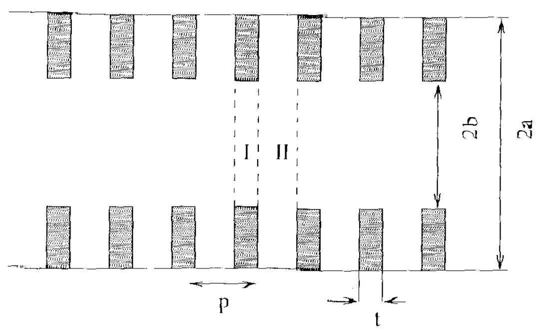

Figure 1: *Cross section and side view of a corrugated circular waveguide*

independent of the angular variable ϕ, we can focus attention on modes with a given angular dependence $\cos(m\phi)$, for example, other modes can be analyzed similarly. The modes of regions I and II are derived from electric and magnetic potentials which we denote by $\Phi_n^{Ite,tm}$ and $\Phi_n^{IIte,tm}$.

The exact transverse electric fields at at $z = 0$, $z = t$ and $z = p$ are denoted by three unknown vector functions $\mathbf{X}_1$, $\mathbf{X}_2$ and $\mathbf{X}_3$, respectively. The Floquet condition is systematically satisfied if we require that

$$\mathbf{X}_3 = e^{-\gamma p}\mathbf{X}_1 \tag{1}$$

where γ is the unknown propagation constant. The remaining unknown functions $\mathbf{X}_1$ and $\mathbf{X}_2$ are expanded in series of the form

$$\mathbf{X}_1 = \sum_{i=1}^{M} c_i^{te}\mathbf{B}_i^{te}(\rho,\phi) + \sum_{i=1}^{M} c_i^{tm}\mathbf{B}_i^{tm}(\rho,\phi) \tag{2}$$

and

$$\mathbf{X}_2 = \sum_{i=1}^{M} d_i^{te}\mathbf{B}_i^{te}(\rho,\phi) + \sum_{i=1}^{M} d_i^{tm}\mathbf{B}_i^{tm}(\rho,\phi). \tag{3}$$

To include the edge conditions at the 90^o-metallic wedges of the corrugations, we introduce the following set of basis functions

$$\mathbf{B}_i^{te} = \frac{\hat{\mathbf{e}}_z \times \nabla_t \Phi_i^{Ite}(\rho,\phi)}{[1-(\frac{\rho}{b})^2]^{1/3}} \tag{4}$$

and

$$\mathbf{B}_i^{tm} = \frac{\nabla_t \Phi_i^{Itm}(\rho,\phi)}{[1-(\frac{\rho}{b})^2]^{1/3}}. \tag{5}$$

In the zero-thickness case, the following basis functions are used

$$\mathbf{B}_i^{te} = \frac{\hat{\mathbf{e}}_\mathbf{z} \times \nabla_\mathbf{t} \Phi_i^{Ite}(\rho, \phi)}{[1 - (\frac{\rho}{b})^2]^{1/2}} \tag{6}$$

and

$$\mathbf{B}_i^{tm} = \frac{\nabla_\mathbf{t} \Phi_i^{Itm}(\rho, \phi)}{[1 - (\frac{\rho}{b})^2]^{1/2}}. \tag{7}$$

By expanding the numerators and denominators in Taylor series in the vicinity of the metallic wedges, it is straightforward to show that these basis functions have indeed the proper edge conditions. To determine the expansion coefficients, we derive two coupled vector integral equations for the functions $\mathbf{X}_1$ and $\mathbf{X}_2$, which are then solved by the moment method. It can be shown that the expansion coefficients satisfy an eigenvalue equation of the form [5]

$$[K]\,[v] + e^{-\gamma p}\,[L]\,[v] = 0. \tag{8}$$

The propagation constants can be straightforwardly determined using standard software packages.

III. RESULTS

The first few basis functions for the 90^o wedge are shown in Figures 2 and 3. Only the basis functions corresponding to unit angular dependence are shown. For comparison, the corresponding unperturbed modes of the of the smaller are also plotted. In all cases, it can be seen that the components normal to the metallic wedge become singular whereas the tangential ones vanish with an infinite slope.

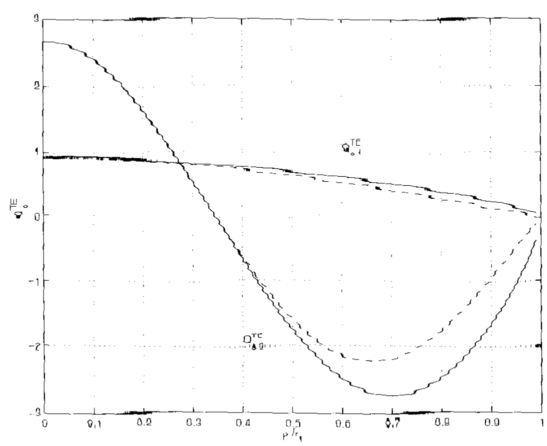

Figure 2: Azimuthal component of the first 2 TE basis functions (solid line). The dashed line shows the corresponding unperturbed modes.

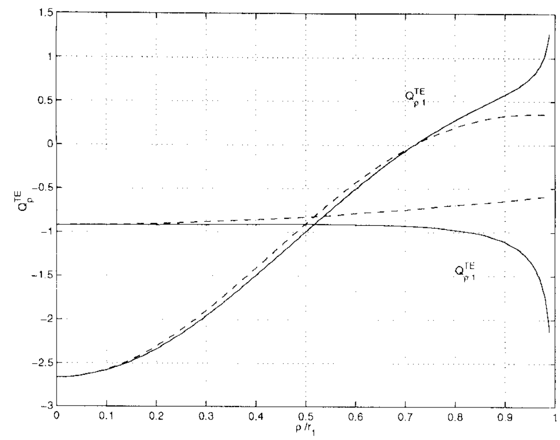

Figure 3: Radial component of the first 2 TE basis functions (solid line). The dashed line shows the corresponding unperturbed modes.

These basis functions were used to compute the dispersion diagram of a large number of corrugated structures. Here we report a representative sample.
Figure 4 shows the results for the H_{01} mode as obtained from the present work. The circles which are experimental results taken from reference [1], are in excellent agreement with the computed results. The data of this figure was generated using 3 basis functions.

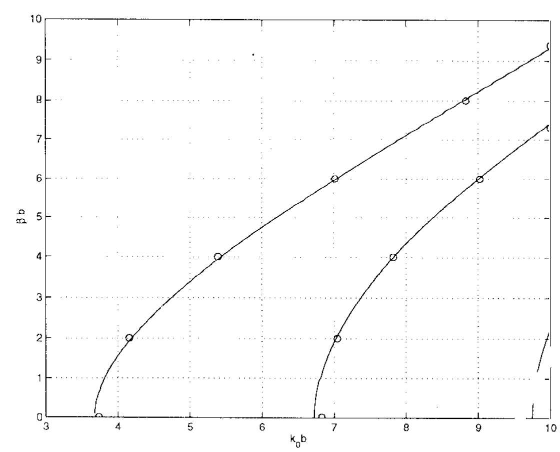

Figure 4: Dispersion curve of H_{01} obtained using 3 basis functions when when $2a$= 7.9423 cm, p =2 cm, $2b$ = 7.112 cm and d = 0.[illegible]449 cm. The circles are experimental results from reference [1].

The case of irises of zero-thickness was also examined using the basis functions above. Excellent agreement is obtained between our results and those presented in reference [2].

We next examine the adequacy of the zero-thickness approximation and limit the discussion to the H_{0n} modes. Figure 5 shows the entire dispersion diagram when $p = a$, $b = 0.6a$ and $d = 1/60$. The solid lines are obtained from the formulation which takes into account the finite thickness of the irises. The dashed lines are the dispersion diagram of the zero-thickness approximation. It is obvious that the two structures have practically identical dispersion diagrams for these dimensions and in this frequency range.

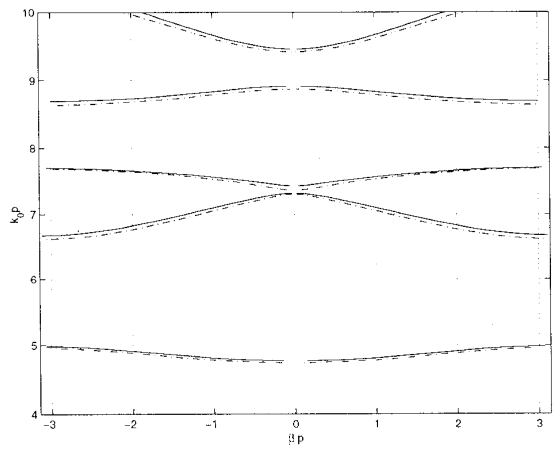

Figure 5: $k_0 - \beta$ diagram of Figure 1, d=a/60 (solid line) and d=0 (dashed line) when $p = a$, $b = 0.6a$.

When the thickness of the irises is increased it is expected that the zero-thickness approximation fails to reproduce the actual propagation properties. Figure 6 shows the dispersion diagram when $p = a$, $b = 0.8a$ and $d = a/8$. The solid lines are the dispersion diagram of the thick irises. The dotted-dashed lines correspond to the zero=thickness approximation. It is obvious that substantial errors would result from the zero-thickness approximation.

From the physics of the problem, we expect that the two discontinuities play a major role in determining the propagation properties of this type of structure. Multiple reflection occur between the two discontinuities separated by a distance d. The zero-thickness approximation fails to take these reflections into account. A better approximation may therefore consist in replacing each of the original thick irises with *two* infinitely thin irises separated by a distance d. Indeed, the dashed lines in Figure 6 show that the dispersion diagram of the resulting structure approximates better that of the thick irises (solid lines) than the standard zero-thickness approximation (dotted-dashed). This observation also suggests that the dispersion diagram of the zero-thickness approximation has less branches than the original structure with thick irises. This point is not addressed in this discussion.

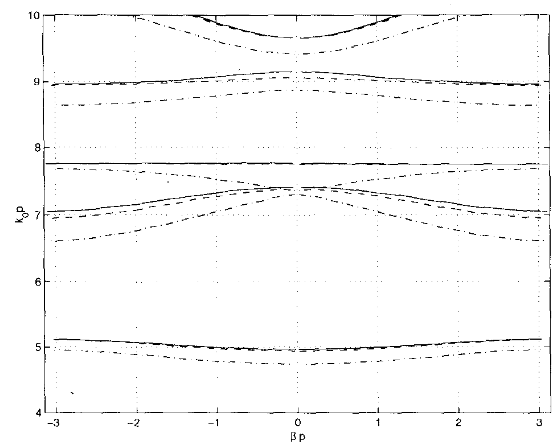

Figure 6: $k_0 - \beta$ diagram of Figure 1 d=a/8 (solid lines) and d=0 (dashed lines) when $p = a$, $b = 0.6a$.

IV. CONCLUSIONS

The propagation constants of Floquet modes are determined from the classical eigenvalues of a generalized matrix eigenvalue problem instead of a determinant equation. A set of edge-conditioned vector basis functions was presented and used to accelerate convergence of the numerical solution. Results obtained form the present work were compared with available data and excellent agreement was documented. Multiple reflections can not be neglected when thick irises are present.

REFERENCES

1 J. B. Davies and B. J. Goldsmith, "An analysis of general mode propagation and the pulse-shortening phenomenon in electron linear accelerators," Philips Res. Repts. 23, pp. 207-232, 1968.

2. P. J. B. Clarricoats and A. D. Olver, Corrugated Horns for Microwave Antennas, Peregrinus, London, 1984.

3. R. E. Collin , Field Theory of Guided Waves, IEEE Press, New York, 1991.

4. S. Amari, J. Bornemann and R. Vahldieck, "Accurate analysis of scattering from multiple waveguide discontinuities using the coupled-integral-equation technique, Jou. Electromag. Waves Appl., vol. 10, pp.1623-1644, Dec. 1996.

5. S. Amari, R. Vahldieck and J. Bornemann, "A new approach to the analysis of periodically loaded circular waveguides," Accepted for publication in IEE Proc. Part H.